Acknowledgment. This investigation was supported in part by Grants-in-Aid for Scientific Research, Cancer Research, and Special Project Research on Cancer-Bioscience from the Ministry of Education, Science, and Culture of Japan.

Registry No. **3**, 113648-22-9; **4**, 113648-23-0; **5**, 130983-86-7; **6**, 113648-24-1; **8**, 119411-03-9; **9**, 119411-04-0; **10**, 130954-02-8; **11**, 130954-03-9; **12a**, 316-46-1; **12b**, 2880-89-9; **12c**, 957-75-5; **12d**, 1024-99-3; **12e**, 1463-10-1; **12f**, 69075-42-9; **12h**, 58-96-8; **13a**, 119411-00-6; **13b**, 129555-74-4; **13c**, 102789-25-3; **13d**, 119422-10-5; **13e**, 130983-87-8; **13f**, 129954-10-5; **13g**, 129532-16-7; **13h**, 69304-38-7; **14a**, 119410-99-0; **14b**, 129555-75-5; **14c**, 119411-02-8; **14d**, 119411-01-7; **14e**, 119410-98-9; **14f**, 129532-13-4; **14g**, 129532-17-8; **14h**, 84828-97-7; **15a**, 129532-06-5; **15b**, 129532-09-8; **15c**, 129555-77-7; **15d**, 129532-11-2; **15e**, 129532-05-4; **15f**, 129532-14-5; **15g**, 129532-18-9; **15h**, 102789-14-0; **16a**, 119410-92-3; **16b**, 119410-96-7; **16c**, 119410-94-5; **16d**, 119410-93-4; **16e**, 119410-90-1; **16f**, 129532-01-0; **16g**, 129532-03-2; **16h**, 119410-95-6; **18a**, 129532-07-6; **18b**, 130954-05-1; **18c**, 129532-10-1; **18d**, 129532-12-3; **18e**, 129532-08-7; **18g**, 129532-19-0; **18h**, 130954-04-0; **19a**, 129531-96-0; **19b**, 129531-98-2; **19c**, 129531-99-3; **19d**, 129532-00-9; **19e**, 129531-97-1; **19g**, 129532-04-3; **19h**, 119804-96-5; **19h**·HCl, 113648-25-2.

Structure–Stability Relationships of Gd(III) Ion Complexes for Magnetic Resonance Imaging

Rune Fossheim,*[†,‡] Harald Dugstad,[‡] and Svein G. Dahl[†]

Institute of Medical Biology, University of Tromsø, N-9001 Tromsø, Norway, and Nycomed AS, P.O. Box 4220 Torshov, N-0401 Oslo 4, Norway. *Received May 11, 1990*

Molecular mechanical calculations and molecular dynamics simulations, based on the AMBER force field, were used to examine the molecular structures and stabilities of nine multidentate ligands and their Gd(III) ion complexes. The magnitude of various factors determining the stability of multidentate Gd(III) complexes, including the energy loss due to change of ligand conformation by complexation, the energy gain from cation–ligand attraction, and effects of intramolecular hydrogen bonding, were calculated by molecular mechanics. The fit between the Gd cation and the binding cavity in the ligands was examined by molecular graphics techniques. Intramolecular hydrogen bonds in free ligands with amide or hydroxyl as H-bond donors usually disfavor complex formation, due to disruption of hydrogen bonds during complex formation. Intramolecular hydrogen bonds may contribute to enhance complex stability if they make the desolvation energy of the free ligands smaller. The calculated complex stabilities were in reasonable agreement with experimental log K values which were available for five of the compounds. The calculated complex stabilities of two hitherto unsynthesized covalently constrained DTPA-derivatives and a DOTA-derivative bearing phenoxy groups as pendant arms indicate that these may form Gd(III) complexes with sufficient stability for use in magnetic resonance imaging techniques.

Introduction

DTPA (1,4,7-triazaheptane-1,1,4,7,7-pentaacetic acid), DOTA (1,4,7,10-tetraazacyclododecane-1,4,7,10-tetraacetate), and other aminopolycarboxylates form highly stable complexes with lanthanide ions.[1] Due to the high magnetic moment of the Gd(III) ion, Gd(III) complexes are widely used as contrast agents in magnetic resonance imaging techniques.[2] Complexation of the gadolinium ion is a prerequisite for diagnostic use since free lanthanide ions are highly toxic. It is important, therefore, that such complexes have high kinetic and thermodynamic stability, in order to prevent their dissociation in the body fluids.

The relationship between complex stability and molecular structure has previously been examined for the aminopolycarboxylate ligands DOTA, DTPA, DO3A (1,4,7,10-tetraazacyclododecane-N,N',N''-triacetic acid), and OTTA (oxa-4,7,10-triazacyclododecane-N,N',N'''-triacetic acid) and their Gd(III) complexes.[3] In the present study, the thermodynamic stabilities of the nine ligands shown in Chart I and their Gd(III) complexes were examined by molecular mechanical calculations and molecular dynamics simulations. One aim of the study was to obtain a model for computation of the stabilities of such complexes, and to evaluate the model from experimental thermodynamic log K values.

Five of the ligands shown in Chart I have previously been synthesized. These include DTPA-BMA (1,7-bis[(N-methylcarbamoyl)methyl]-1,4,7-triazaheptane-1,4,7-triacetic acid),[4] DTPA-HMA ((*S,S*)-2,6-bis(hydroxymethyl)-1,7-bis[(N-methylcarbamoyl)methyl]-1,4,7-triazaheptane-1,4,7-triacetic acid),[4] DTPA-BMPA (1,7-bis[[N-(2,3-dihydroxypropyl)-N-methylcarbamoyl]methyl]-1,4,7-triazaheptane-1,4,7-triacetic acid),[4] TETA (1,4,8,11-tetraazacyclotetradecane-1,4,8,11-tetraacetic acid),[5] and NOTA (1,4,7-triazacyclononane-N,N',N''-triacetic acid).[5] The other four compounds have not been synthesized. DTPA-TRANS (*trans*-2,6-bis[[N,N-bis(carboxymethyl)amino]methyl]piperidine-N-acetic acid), DTPA-CIS (*cis*-2,6-bis[[N,N-bis(carboxymethyl)amino]methyl]piperidine-N-acetic acid), PHEA (1,4,7-tris(2-hydroxyphenyl)-1,4,7,10-tetraazacyclododecane), and DTPA-HB (1,4,7-triazaheptane-1,1,4,7,7-pentakis[bis(hydroxy methyl)acetic acid]) were included as model compounds in order to examine structural effects on Gd(III) complex stabilities. DTPA-HB was included in the calculations in order to investigate effects of hydrogen bonding on complex stability. PHEA was included in order to investigate the ligating strength of phenoxy groups, and DTPA-CIS and DTPA-TRANS were included in order to compare the Gd(III) complex stabilities of these two isomers with that of DTPA.

The binding cavities in the NOTA, TETA, DOTA, and DTPA-HMA complexes were mapped by molecular graphics techniques, in order to investigate to what extent cation–cavity size fit determines the stability of Gd(III)

[†] University of Tromsø.
[‡] Nycomed AS.

(1) Desreux, J. F.; Barthelemy, P. P. *Nucl. Med. Biol.* **1983**, *15*, 9.
(2) Lauffer, R. B. *Chem. Rev.* **1987**, *87*, 901.
(3) Fossheim, R.; Dahl, S. G. *Acta Chem. Scand.* **1990**, *44*, 698.
(4) DTPA-BMA: US. Pat. 4687659, 1984; DTPA-HMA: Eur. Pat. 299795, 1987; and DTPA-BMPA: Eur. Pat. 130934, 1983.
(5) Desreux, J. F. *Inorg. Chem.* **1980**, *19*, 1319.

0022-2623/91/1834-0819$02.50/0

Chart I

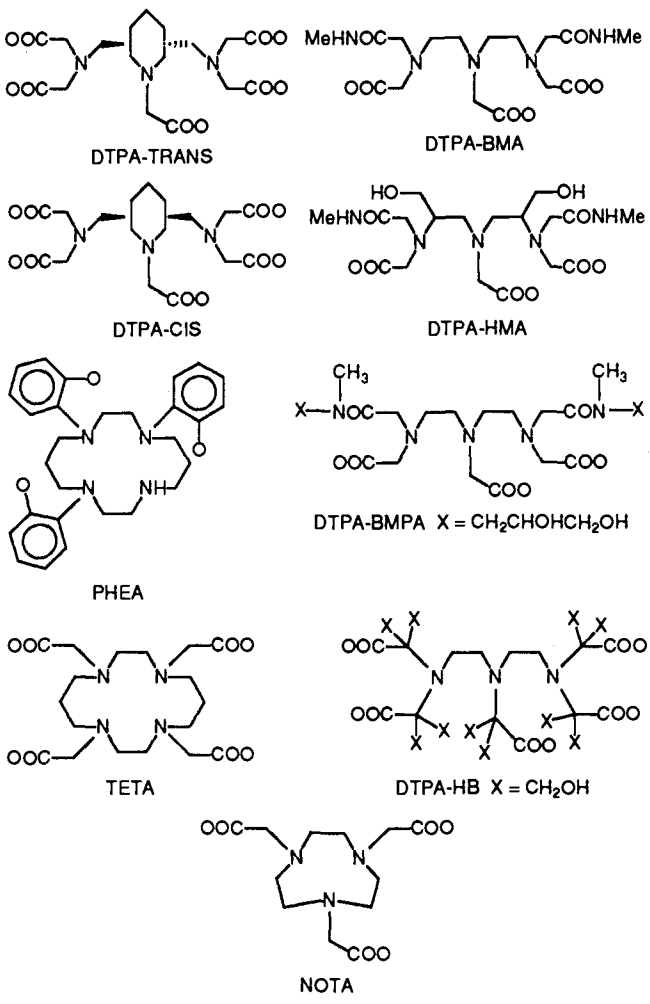

complexes. The four compounds were chosen in order to investigate differences between cyclic and noncyclic ligands and between cyclic ligands with different ring sizes.

Methods

Molecular mechanical calculations and molecular dynamics simulations were performed with the AMBER software package[6] on a VAX 8600/VMS system. The MIDAS programs[7] were used for molecular graphics on an Evans and Sutherland PS390 workstation with a MicroVax II/Ultrix system as host computer.

Atomic Point Charges. Atomic point charges,[8] which were used as parameters in molecular mechanical calculations and molecular dynamics simulations, were obtained from ab initio calculations with the QUEST 1.0 program,[8] which is based on the GAUSSIAN-80 program.[9] QUEST calculates quantum mechanical electrostatic potentials in a number of layers around the molecule, and net atomic point charges by least-squares fitting to the electrostatic potentials. Electrostatic potentials in four layers 0.2 Å apart, the inner-most layer corresponding to 1.4 times the van der Waals radii, and atomic point charges were calculated on a CRAY X-MP computer with use of a STO-3G basis set.

Due to the size of the molecules, the atomic charge calculations of all ligands except NOTA were performed on two or three overlapping fragments of each ion, and the charges on overlapping atoms were adjusted in order to give the correct total charge of the ion. The charge calculations for DTPA-TRANS, TETA and PHEA were performed on two fragments of the ions. For DTPA-TRANS the charge calculations were performed on *trans*-2-[[*N*,*N*-bis(carboxymethyl)amino]methyl]-6-methylpiperidine-*N*-acetic acid and [[*N*,*N*-bis(carboxymethyl)amino]methyl]ethylamine. For TETA the charge calculations were performed on 2,5,9-triazadecane-2,5,9-triacetic acid and 3-azahexane-3-acetic acid. For PHEA the charge calculations were performed on 2,5-bis(2-hydroxyphenyl)-2,5-diazahexane and on 3-(2-hydroxyphenyl)-3,6-diazaoctane. Atomic point charges calculated for DTPA-TRANS were also used for the DTPA-CIS isomer. The charges for DTPA-BMA and DTPA-BMPA were derived from previous calculations on DTPA,[3] assigning common atoms the same charges as in DTPA. The charges for the amide groups were obtained by charge calculations on the corresponding acetamides. Charges for DTPA-HB were derived from the DTPA charges and from a charge calculation on bis(hydroxymethyl)acetate. Charges for DTPA-HMA were derived from the charges calculated for DTPA-BMA and the hydroxymethyl charges calculated for bis(hydroxymethyl)acetate.

Geometry Optimization and Molecular Dynamics of Free Ligands. Starting coordinates for TETA were obtained from the crystal structure of Na[TbTETA].[10] Starting coordinates for NOTA, DTPA-CIS, and DTPA-TRANS were obtained by model building, with values for bond lengths and bond angles taken from similar structures.[3] Two starting conformers of DTPA-TRANS were made, one with the N substituent of the chair-conformation piperidine ring in axial position and the other with the N substituent in equatorial position. Four starting conformers of DTPA-CIS were made by model building. These correspond to the four possible combinations of axial and equatorial ring substituents in a piperidine chair conformer. A starting structure for PHEA was made by substitution of CH_2COO in DO3A[3] with phenoxy groups, and starting structures for DTPA-BMA, DTPA-HMA, and DTPA-BMPA were made by appropriate acetamide and hydroxymethyl substitutions in DTPA. A starting structure for DTPA-HB was made by substitutions of 10 hydroxymethyl groups in DTPA (Chart I).

The following calculations were performed on each of the nine ligands. (1) In order to obtain reasonable models for the charge calculations, the starting structures were first optimized by energy minimizations in vacuo without including electrostatic interactions. (2) Atomic point charges were calculated for these structures. (3) The structures were reoptimized in vacuo including electrostatic interactions. (4) The reoptimized ligand structures were used as starting points for 10-ps molecular dynamics simulations in vacuo at 300 K, after an initial 1-ps equilibration period during which the temperature was raised from 0.1 to 300 K. The coordinates were stored 100 times during each 10-ps simulation. (5) From the structrues sampled in each molecular dynamics simulation, the three having lowest potential energy were selected and refined by energy

(6) Singh, U. C.; Weiner, P. K.; Caldwell, J. W.; Kollman, P. A. *AMBER (UCSF Version 3.0)*; Department of Pharmaceutical Chemistry, University of California: San Francisco, CA, 1986.
(7) Ferrin, T. E.; Huang, C. C.; Jarvis, L. E.; Langridge, R. *J. Mol. Graphics* **1988**, *6*, 13.
(8) Singh, U. C.; Kollman, P. A. *J. Comp. Chem.* **1984**, *5*, 129.
(9) Binkley, J. S.; Whiteside, R. A.; Kirshnan, R.; Seeger, R.; Defrees, D. J.; Schlegel, H. B.; Topiol, S.; Kahn, L. R.; Pople, J. A. *GAUSSIAN 80*, Quantum Chemistry Program Exchange, 1980.
(10) Spirlet, M.-R.; Rebizant, J.; Loncin, M.-F.; Desreux, J. F. *Inorg. Chem.* **1984**, *23*, 4278.

minimization. (6) In order to examine hydration effects, the lowest-energy conformers were submerged in a layer of water with thickness 8 Å, containing approximately 200 randomly distributed water molecules. The energy of the solute and solvent was minimized by using a water oxygen charge of $Q_{OW} = -0.66$. This oxygen charge has been found to give reasonable water/chromophore hydrogen bonding energies.[11]

The energy minimizations in aqueous solution were performed with a constant dielectric function, $\epsilon = 1.0$. All in vacuo calculations were performed with a distant dependent dielectric function, $\epsilon = r_{ij}$, where r_{ij} is the interatomic distance.

Geometry Optimization and Molecular Dynamics of Gd Complexes. In calculations on Gd(III) complexes the cation charge +3 and the van der Waals radius $R_{Gd} = 1.8$ and a van der Waals well-depth $e_{Gd} = 0.2$ were used as nonbonded gadolinium parameters.[3] Only nonbonded parameters were used to describe the interaction between ligand and cation, i.e. bond, angle, and torsional terms involving Gd were set equal to zero. Amine nitrogen charges of −0.4 were used instead of the calculated ligand nitrogen charges, which were in the range −0.1 to −0.3, and excess charge was distributed on adjacent carbon atoms. A nitrogen atomic charge of −0.4 was previously found to give the best agreement between calculated Gd–N and Gd–O distances and X-ray crystallographic results.[3]

A starting geometry for the GdTETA complex was obtained from the crystal structure of Na[TbTETA].[10] Starting geometries for the other complexes were obtained with the computer graphics system, by adjusting the ligand torsion angles in order to obtain full coordination and Gd–ligand atom distances close to corresponding distances in other aminopolycarboxylate complexes.[3] Since the terminal amine N atoms become chiral in the complexes of the three bisamides DTPA-BMA, DTPA-HMA, and DTPA-BMPA, models were built of the (*S*,*R*), (*R*,*S*), and (*R*,*R*) isomers of DTPA-BMA and DTPA-HMA. Furthermore, since the crystal structure of the bis(ethylamide) analogue of DTPA-BMA is available (DTPA-BEA),[12] a starting geometry for DTPA-BMA was also obtained by replacing the two methyl groups with hydrogen atoms. The complexes were energy minimized in vacuo, and each complex structure was then submerged in a layer of water with thickness 8 Å, and the energies of the solute-solvent systems were refined.

The layers of water were then removed and energy minimizations performed on GdNOTA·3H_2O and on monohydrated complexes of the other ligands. For water oxygens a charge of $Q_{OW} = -0.7$ and van der Waals radius $R^*_{OW} = 1.67$ were used in the calculations. These parameters have been found to give reasonable agreement between experimental and calculated total hydration energies of Gd(III).[3] A constant dielectric function, $\epsilon = 1.0$, was used in the energy minimizations with water solvent. Energy minimizations in vacuo were performed with a distance dependent dielectric function, as for the free ligands.

In order to compare the complex stabilities of GdDTPA-CIS and GdDTPA-TRANS, molecular dynamics simulations and energy minimizations of the two monohydrated isomeric complexes were performed as described under 4 and 5, above. Furthermore, the DTPA ligand was constrained to the lowest energy conformations of DTPA-CIS and DTPA-TRANS, respectively, and energy minimizations were performed on GdDTPA·H_2O, keeping the ligand in these conformations. This was accomplished by using high constrain energy force constants ($K = 10000$) for the torsion angles.

Complex stabilities were derived from the calculated reaction energies in vacuo and in an aqueous environment. The reaction energy in vacuo was calculated by eq 1. E_{ML}

$$E_{r,g} = E_{ML} - E_L \quad (1)$$

is the energy of the complex (ligand and cation), and E_L is the energy of the free ligand in the lowest energy conformer found. The reaction energy may also be expressed as in eq 2. E_i is the interaction energy between cation and

$$E_{r,g} = E_i + E_{d,l} \quad (2)$$

ligand. $E_{d,l}$ is the ligand constrain energy, defined as the difference between the energy of the ligand in the complex conformation and the lowest energy of the free ligand. The reaction energy in aqueous solution was calculated by considering two hydration effects, hydration of the carboxylate, amide, and phenoxy groups (E_{h1}) and hydration of the lanthanide ion by occupation of vacant coordination sites in the complexes (E_{h2}). The reaction energy in an aqueous environment was calculated as in eq 3.[3]

$$E_{r,aq} = E_{r,g} + E_{h1} + E_{h2} \quad (3)$$

Binding Cavities. The binding cavities of the ligands NOTA, DOTA, TETA, and DTPA-HMA were investigated by molecular graphics techniques, from Connolly surfaces[13] generated for the ligands in their complex conformations. The Connolly surfaces are defined by rolling a sphere over the van der Waals surface of the ligand, with the contact reentry points used to determine the surface. By using a sphere with radius 1.0 Å, corresponding to the ionic radius of Gd(III),[14] the "lanthanide ion accessible surface" of each ligand was mapped by this procedure. This surface describes the topography of the binding cavity available for a Gd(III) ion in a particular ligand conformation. The surfaces were displayed with the MIDAS programs,[7] in order to visualize the size and shape of the binding cavities.

Results

The energies of the lowest-energy conformers of the ligands and of mono- and trihydrated complexes are given in Table I. Stereographic drawings of the ligands NOTA, TETA, DTPA-BMA, and DTPA-HMA in their lowest-energy conformations are shown in Figure 1. The structures of Gd(III) complexes with PHEA, DTPA-BMA, DTPA-CIS, and DTPA-TRANS are shown in Figure 2. The corresponding coordination polyhedra for the structures are shown in Figure 3. These structures are shown in order to illustrate various adopted ring conformations, effects of hydrogen bonding on ligand conformation, and differences in coordination geometry. The hydration energies and reaction energies of the nine compounds in vacuo and in aqueous solution are given in Table II.

Ligands. The nine-membered NOTA ring adopted a [12222][15] "pentagon" conformation having pseudo-C_2 symmetry in the lowest-energy conformer, with the carboxylate groups pointing to both sides of the ring plane

(11) Weiner, S. J.; Kollman, P. A.; Case, D. A.; Singh, U. C.; Ghio, C.; Alagona, G.; Profeta, S.; Weiner, P. *J. Am. Chem. Soc.* **1984**, *106*, 765.
(12) Konigs, M. S.; Dow, W. C.; Love, D. B.; Raymond, K. N.; Quay, S. C.; Rocklage, S. M. *Inorg. Chem.* **1990**, *29*, 1488.
(13) Connolly, M. L. *Science* **1983**, *221*, 709.
(14) Shannon, R. D. *Acta Cryst.* **1976**, *A32*, 751.
(15) Dale, J. *Isr. J. Chem.* **1980**, *20*, 3.

Table I. Ligand and Complex Energies (kcal/mol) and Type of Coordination Polyhedra (CP) in Nine-Coordinated Hydrated Complexes

compd	ligand energy	complex energy				
	total (E_l)	total (E_t)	ligand constrain (E_{dl})	ligand–cation (E_i)	hydration (E_h)	CP[a]
NOTA	23.8	-334.8	41.1			
NOTA·3H_2O		-404.3	40.1	-391.5	-27.2, -27.3, -27.3	UNS
TETA	46.4	-373.0	102.0			
TETA·H_2O		-388.2	98.9	-514.2	-19.5	TTP
DTPA-CIS	57.6	-429.2	146.4			
DTPA-CIS·H_2O		-446.7	144.8	-628.2	-21.3	TTP
DTPA·H_2O[b]	67.4	-425.2			-21.1	
DTPA-TRANS	59.0	-426.7	136.0			
DTPA-TRANS·H_2O		-443.8	133.6	-618.1	-18.8	TTP
DTPA·H_2O[c]	67.4	-425.4			-18.6	
DTPA-BMA	-9.9	-364.6	108.5			
DTPA-BMA·H_2O		-385.5	108.5	-460.2	-24.2	TTP
DTPA-BMPA	2.7	-361.6	91.6			
DTPA-BMPA·H_2O		-381.4	105.2	-464.7	-24.8	UNS
DTPA-HMA	-7.8	-349.6	123.6			
DTPA-HMA·H_2O		-375.6	113.4	-462.0	-22.2	UNS
PHEA	46.5	-310.2	37.8			
PHEA·2H_2O		-357.0	39.3	-391.0	-25.6, -22.9	MSA
DTPA-HB	89.9	-311.8	118.3			
DTPA-HB·H_2O		-333.3	165.3	-566.6	-21.5	UNS

[a] TTP = tricapped trigonal prisms; MSA = monocapped square antiprisms; UNS = no apparent symmetry found in the energy minimized structures. [b] Energies of DTPA·H_2O constrained to the same complex conformation as that of DTPA-CIS. [c] Energies of DTPA·H_2O constrained to the same complex conformation as that of DTPA-TRANS.

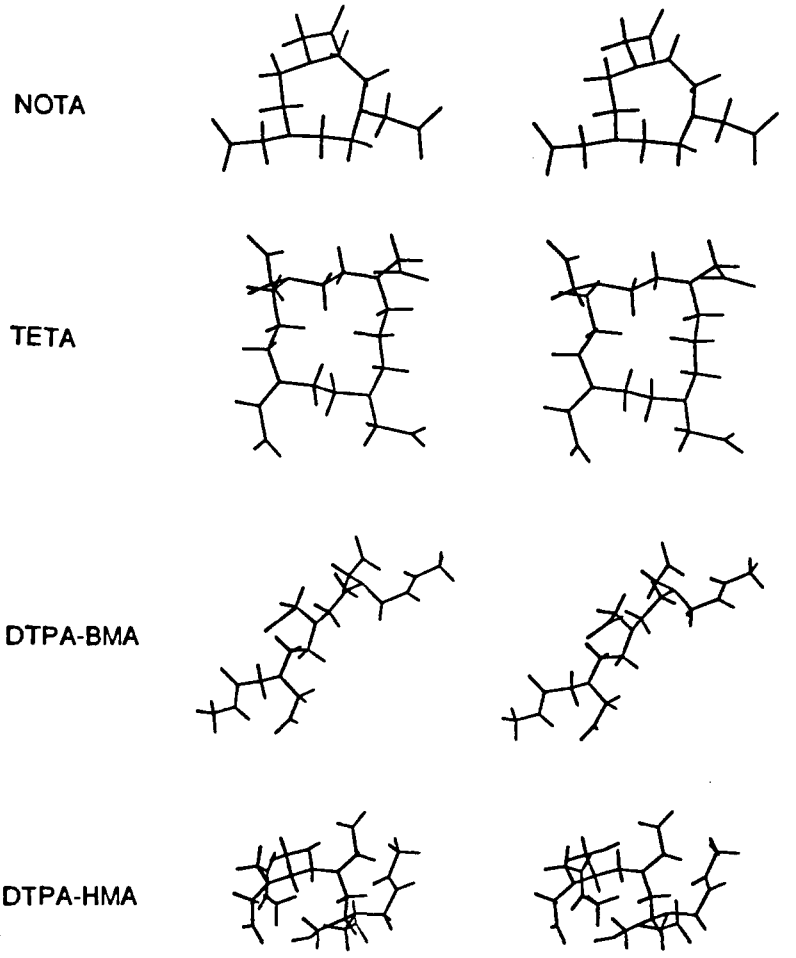

Figure 1. Stereoscopic drawings of NOTA, TETA, DTPA-BMA, and DTPA-HMA free ligands.

as shown in Figure 1. This conformation had 4.5 kcal/mol lower energy than the D_3 "triangle" conformation [333], which was also adopted in the geometry optmized GdNOTA complex. In the 14-membered TETA ring a [3434] "quadrangular" conformation with the nitrogen atoms placed at the corners had lowest energy (Figure 1). The lowest-energy conformer of PHEA adopted an unsymmetric conformation of the 12-membered ring. Comparison of the free-ligand conformers of DTPA-HMA and DTPA-BMA, which had lowest energy, shows that DTPA-HMA has a more globular shape than DTPA-BMA (Figure 1). In DTPA-HMA two hydroxyl groups and two amide nitrogen atoms act as hydrogen-bond acceptors from carboxylate groups. In DTPA-BMA the two amide ni-

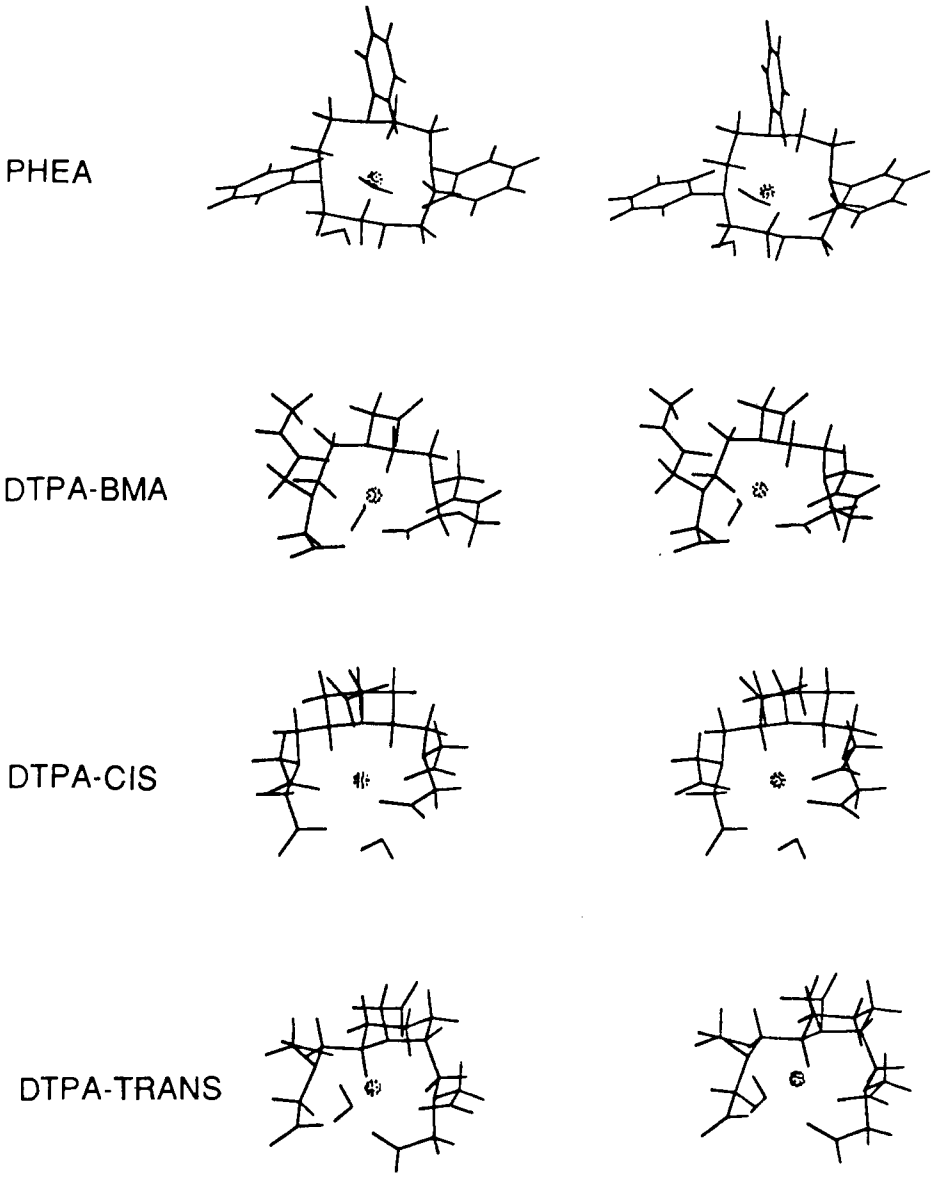

Figure 2. Stereoscopic drawings of PHEA, DTPA-BMA, DTPA-CIS, and DTPA-TRANS complexes.

Table II. Hydration and Reaction Energies (kcal/mol) by Gd(III) Complex Formation in Vacuo and in Aqueous Solution

ligand	reaction energy in vacuo ($E_{r,g}$)	hydration of -COR[a] (E_{h1})	hydration of complex (E_{h2})	reaction energy in water ($E_{r,aq}$)
NOTA	-351.4	77.6	-71.4 (54.5)[b]	-345.2 (328.3)[b]
TETA	-415.3	82.4	-29.9	-362.8
DTPA-CIS	-483.4	148.9	-31.7	-366.2
DTPA-TRANS	-484.4	157.9	-29.2	-355.7
DTPA-BMA	-351.6	45.3	-34.6	-340.9
DTPA-BMPA	-359.4	56.2	-35.2	-338.4
DTPA-HMA	-345.9	39.7	-32.6	-341.7
PHEA	-351.7	63.9	-54.6	-342.4
DTPA-HB	-401.1	141.3	-31.9	-291.7

[a] Differences in hydration energies between free ligand and complex of the carboxylate (R = O), amide (R = NX_2), and phenoxy groups (R = none). [b] GdNOTA may coordinate three water molecules. Energies in parentheses are calculated for two coordinated water molecules.

trogen atoms are hydrogen bonded to carboxylate groups in the same parts of the molecule.

The piperidine ring in the isomers DTPA-CIS and DTPA-TRANS had a chair conformation in all low-energy conformers examined. The lowest-energy conformer of DTPA-CIS had all three ring substituents in equatorial positions. In DTPA-TRANS, the trans configuration forces one piperidine ring substituent into an axial position.

Gd(III) Complexes. Most of the coordination polyhedra of the nine mono- and trihydrated complexes may be classified as pseudo tricapped trigonal prisms (TTP) or as monocapped square antiprisms (MSA), as indicated in Table I and illustrated in Figure 3. Both the DTPA-CIS and DTPA-TRANS isomers had tricapped trigonal prismatic coordination polyhedra. The isomers differ in coordination geometry since the caps are formed by two carboxylate oxygens and one nitrogen in DTPA-CIS and by two nitrogen atoms and oxygen (water) in DTPA-TRANS. The energy minimized GdDTPA·H_2O complex also adopted a tricapped trigonal prismatic coordination geometry, in agreement with crystal structure data for the Ba[NdDTPA]·H_2O complex.[16]

The isomers of DTPA-BMA and DTPA-HMA with lowest energy had the same chirality (*R,S*) and the same chirality as the isomer found in the crystal structure of the analogue bis(ethylamide).[12] This isomer has both the coordinating amide groups in neighboring positions to the central carboxylate group as shown in Figure 2, thus maximizing charge separation between the negatively

(16) Stezowski, J. J.; Hoard, J. L. *Isr. J. Chem.* 1984, *24*, 323.

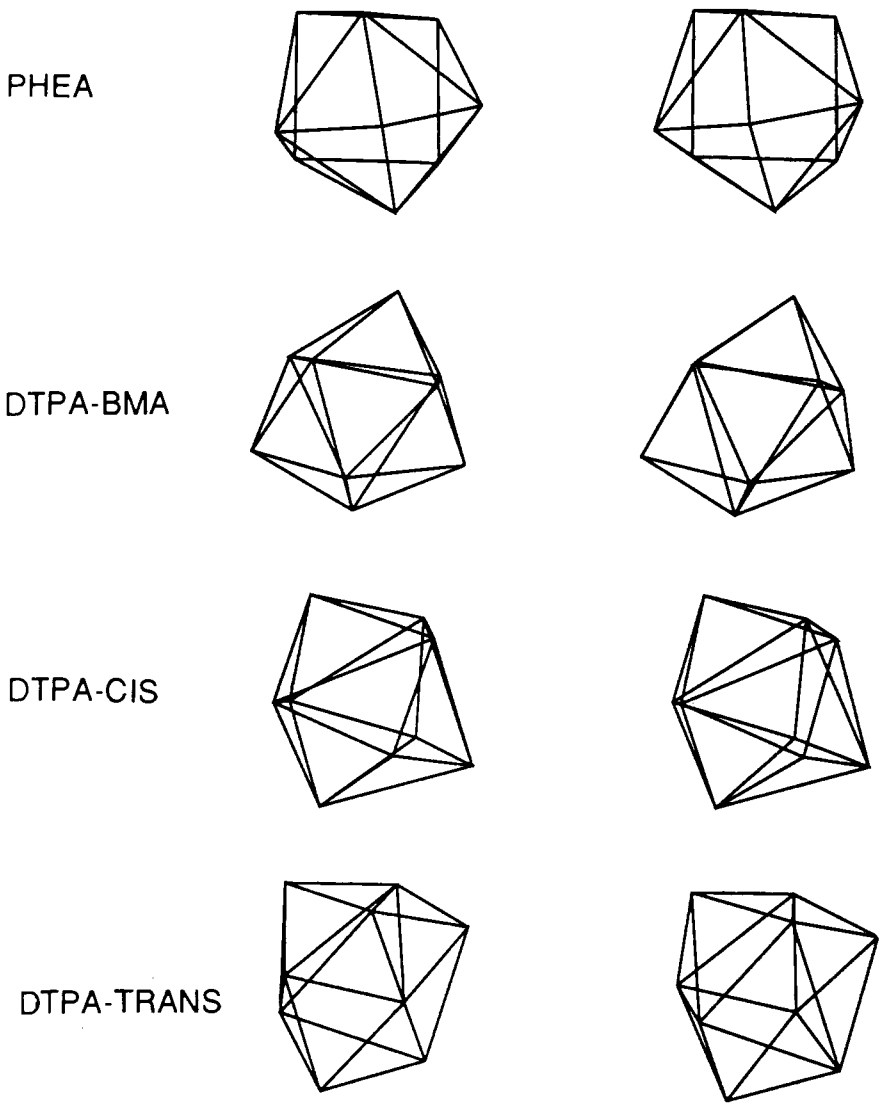

Figure 3. Stereoscopic drawings of PHEA, DTPA-BMA, DTPA-CIS, and DTPA-TRANS coordination polyhedra.

charged carboxylate groups in the complexes. The isomer having the terminal carboxylate groups in these positions (*S,R*) is calculated to be 4.8 and 9.4 kcal/mol less stable for DTPA-BMA and DTPA-HMA, respectively. Corresponding values for the isomer having one carboxylate group and one amide group in these positions (*R,R*) is 5.7 and 4.5 kcal/mol. The structure of DTPA-BMA energy minimized from the modeled coordinates had a square antiprismatic coordination geometry, as opposed to the trigonal prismatic coordination geometry found in the DTPA-BEA crystal structure,[12] and in the structure energy minimized from these crystal coordinates. However, the energy difference between the conformers is only 2.5 kcal/mol in favor of the latter, which may suggest that both these two coordination geometries are accessible in solution.

Figure 4 shows the total cation–ligand interaction energy (E_i) as a function of the ligand constrain energy ($E_{d,l}$) in 13 different Gd(III) complexes. A fair linear relationship was found between these parameters (r = 0.84). All complexes with eight ligating atoms (solid circles) lie above those with seven ligating atoms (open circles). NOTA, which has six ligating atoms, lies closest to the origin. Within each group, the position along the line seems to be determined mainly by ligand type. In Figure 4 compounds with five carboxylate groups (DTPA-CIS, DTPA-TRANS, DTPA, and DTPA-HB) lie above those with four

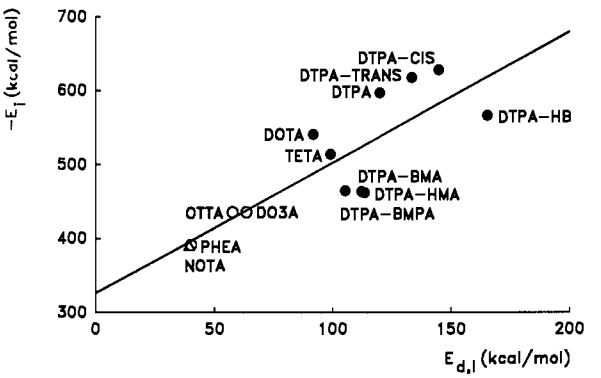

Figure 4. Relationship between total ligand–cation interaction energy (E_i) and ligand constrain energy ($E_{d,l}$). Solid circles indicates compounds with eight ligating atoms. Open circles indicate compounds with seven ligating atoms. Open triangle indicates the compound with six ligating atoms. Regression line: $-E_i = 1.76E_{d,l} + 326.8$, r = 0.84.

carboxylate groups (DOTA and TETA), which lie above those with three carboxylate groups (DTPA-BMA, DTPA-HMA, and DTPA-BMPA) on the y axis.

Figure 5 shows the relationship between calculated reaction energies in an aqueous environment and previously reported experimental thermodynamic log K values of GdDOTA,[17] GdDTPA,[17,18] GdDO3A,[18] GdNOTA,[17] and

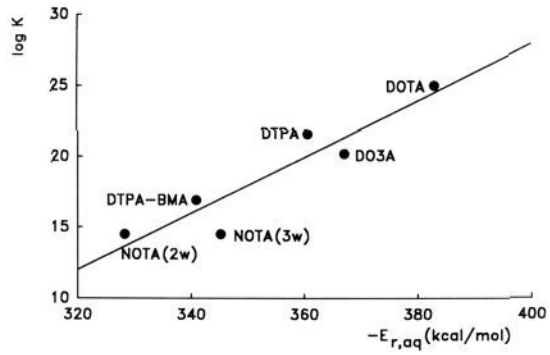

Figure 5. Relationship between reaction energies in water ($E_{r,aq}$) and experimental log K values. The two points given for NOTA are calculated assuming two (2w) and three (3w) coordinated water molecules in the complex. Regression line: $\log K = -0.20E_{r,aq} - 51.5$, $r = -0.93$.

GdDTPA-BMA.[19] Reaction energies of NOTA were calculated both with two and three coordinated water molecules. A linear relationship between experimental log K values and calculated reaction energies was found, indicating that semiquantitative predictions of complex stability may be made from this type of calculations.

DTPA-BMA had slightly lower reaction energy in vacuo than DTPA-HMA (Table II). However, the reaction energies in aqueous solution are similar for the two compounds. In the free DTPA-HMA ligand the carboxylate groups are partly shielded from the water phase by intramolecular hydrogen bonding to the hydroxyl groups. In the complex conformation of DTPA-HMA the hydroxyl groups are unavailable for hydrogen bonding to the uncoordinated carboxylate oxygens. This makes the desolvation energy of the carboxylate groups (E_{hl}) smaller in DTPA-HMA than in DTPA-BMA (Table II), which suggests that complex formation will be favored in DTPA-HMA by this desolvation effect.

Unsynthesized Complexes. In DTPA-HB all α-carboxyl hydrogens in DTPA are replaced by hydroxymethyl groups, thus making a number of intramolecular hydrogen bonding patterns possible. In the geometry-optimized free-ligand structure of DTPA-HB in water 3.1 hydrogen bonds to water molecules were formed per oxygen (carboxylate), compared to 3.7 in the DTPA ligand. This shows that the carboxylate groups of DTPA-HB would be shielded, an effect which was also seen in the Gd(III) complex. In the geometry-optimized GdDTPA-HB complex only 2.1 hydrogen bonds were formed per uncoordinated oxygen (carboxylate), compared to 3.6 in the GdDTPA complex. In this case the calculated hydration effects seem to disfavor complex formation.

The calculated coordination polyhedra for DTPA-CIS and DTPA-TRANS (Table I) suggest that both ligands may form stable lanthanide ion complexes. This is supported by the finding that when DTPA is constrained to the DTPA-CIS and DTPA-TRANS complex conformations, respectively, the two conformers had similar energies (Table II), which were only slightly lower than the energy of Gd[DTPA]·H_2O, energy minimized without constraints (−428.6 kcal/mol).[3] The reaction energies in vacuo indicate that the two isomers have similar stabilities and are slightly more stable than DTPA (−476.7 kcal/mol).[3] The reaction energies, which were calculated when hydration effects were incorporated, indicate that DTPA-CIS is more stable than DTPA ($E_{r,aq}$ = −360.5 kcal/mol),[3] and that DTPA is more stable than DTPA-TRANS (Table II).

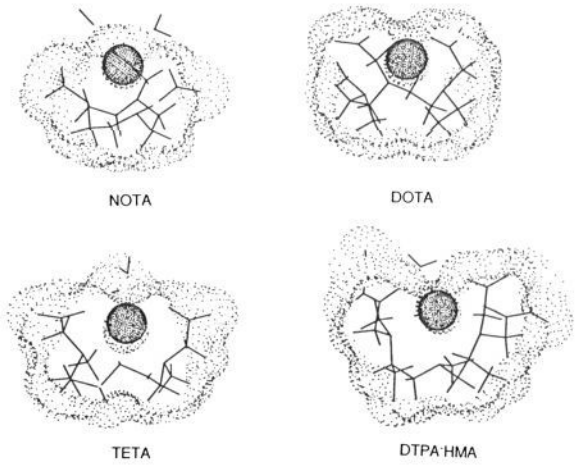

Figure 6. Gd(III) accessible surface of NOTA, DOTA, TETA, and DTPA-HMA. The Gd(III) ion is illustrated as a sphere with radius 1 Å. Clipping planes have been used to enhance viewing of the cavity size.

The reaction energy in vacuo was slightly larger for PHEA than for DTPA-HMA and DTPA-BMA, both of which have one more ligating atom. The reaction energies in an aqueous environment are also consistent with this order of stabilities of the complexes, with PHEA slightly more stable than both the bis-amides, DTPA-BMA, and DTPA-HMA.

Binding Cavities. The structures and Gd(III) accessible surfaces of NOTA, DOTA, TETA, and DTPA-HMA are shown in Figure 6. There was a distinct difference in cavity shape and size among the cyclic ligands NOTA, DOTA, and TETA. In NOTA the cavity was shallow, leaving about half of the cation exposed to the surrounding water phase. Consistent with this, the NOTA complex is the least stable among the three, judged from available log K values.[17] The larger DOTA ring is the one among the three cyclic ligands which best incorporates a Gd(III) ion. This compound also has the highest log K value of the three.[17] The binding cavity in TETA is larger than that in DOTA in the direction toward the center of the ring, which shows the effect of the size of the macrocyclic ring on the size of the cavity. In the case of the three cyclic ligands the degree of cation–cavity fit correlates well with complex stability. However, DTPA-HMA has a Gd(III) accessible cavity that fits the cation equally well compared to DOTA, while the DOTA and DTPA bis(methylamide) complexes differ by a factor 10^7 in log K values.[17,19] Therefore, the binding cavity available for a Gd(III) ion in the complex conformation of a ligand only gives a certain indication of the stability of the complex.

Discussion

The molecular modeling calculations presented here illustrate and quantify several of the factors which are important for the stability of multidentate Gd(III) complexes. Judging from the positioning of compounds along the regression line shown in Figure 4, the number of ligating atoms and their type is clearly important for the stability of Gd(III) complexes. However, a gain in ligand–cation attraction energy, which may be obtained by

(17) Cacheris, W. P.; Nickle, S. K.; Sherry, A. D. *Inorg. Chem.* **1987**, *26*, 958.
(18) Tweedle, M. F.; Gaughan, G. T.; Chang, C. A.; Hagan, J. J. *Book of Abstracts*. Society of Magnetic Resonance in Medicine, Seventh Annual Meeting and Exhibition, San Francisco, CA, 1988, p 788.
(19) Cacheris, W. P.; Quay, S. C.; Rocklage, S. M. *Magn. Reson. Imaging* Submitted for publication.

increasing the number of ligating atoms and using strong ligating groups, is accompanied by larger ligand–ligand repulsion in the complex. Since the regression line shown in Figure 4 has a slope larger than unity (1.76), the gain in ligand–cation energy is usually not outweighed by the increased ligand–ligand repulsion energy.

The x and y axis in Figure 4 represent two opposing energy contributions to the in vacuo stabilities of the complexes. The position of a compound in this figure gives an indication of its complex stability. Predictions of complex stabilities may also be made from the regression line shown in Figure 5 which relates experimental log K values to calculated $E_{r,aq}$ values. The position of a compound in relation to the regression line in Figure 4 indicates whether conformational features of the ligands favors or disfavors complexation. In compounds lying far above the line, conformational features of the ligands will favor complexation, compared to the compounds below the line. The compounds above the regression line in Figure 4 include DOTA and DTPA, which form Gd complexes among the most stable which are known.[1,2] In compounds lying below the regression line, conformational features of the ligands disfavor complexation compared to those above the line.

A common feature of all compounds below the regression line in Figure 4 is the presence of intramolecular hydrogen bonds in the free ligands, where amides or hydroxyl groups act as donors and carboxylate groups as acceptors. In most cases, these hydrogen bonds are disrupted during complex formation. Intramolecular hydrogen bonding appears to disfavor complexation of DTPA-HMA and DTPA-BMA to approximately the same extent, since the ligand constrain energy (E_{dl}) is similar for the two compounds (Table I). The results of the present calculations suggest that intramolecular hydrogen bonds may both increase and decrease complex stability. As depicted in Figure 4, disruption of intramolecular H-bonds during complex formation generally decreases the complex stability. On the other hand, intramolecular H-bonds may contribute to enhance complex stability if they make the desolvation energy of the free ligands smaller, as suggested by the results of the calculations on the bisamides DTPA-BMA and DTPA-HMA.

log K values of 28.2 and 15.75 have been reported for EuDOTA and GdTETA,[20] respectively. Since at least the former value is disputed,[17] these have not been included in Figure 5. The log K value of GdTETA suggests that the complex is less stable than predicted from the model. However, TETA clearly has lower complex stability than DOTA, judging from their respective $E_{r,aq}$ values (Table II).

Energy minimization of the TETA complex with solvent water indicated that the lanthanide ion is less accessible to water coordination in this complex than the others. The shortest Gd(III)–O (water) distance (2.94 Å) was approximately 0.4 Å longer than the distances usually found in energy minimized hydrated Gd(III) complexes. No coordinating water molecules were found in the Na[TbTETA]·$6H_2O$ crystal structure,[10] and it has been claimed that this situation also prevails in solution.[1] However, solution studies of the EuTETA complex by the luminescence method indicate a water coordination number of 0.6.[21] In our calculations the GdTETA·H_2O complex energy minimized in vacuo was nine-coordinate, with a tricapped trigonal prismatic coordination geometry. This is different from the distorted dodecahedral coordination geometry observed in the crystal.

The results of the calculations on the hitherto unsynthesized compounds DTPA-CIS, DTPA-TRANS, and PHEA indicate that all three may form Gd(III) complexes which are sufficiently stable to be interesting candidates for magnetic resonance imaging techniques. The energy differences between DTPA-CIS and DTPA-TRANS were generally small, and do not permit a clear distinction regarding their complex stability. Judging from structure and energy data, both isomers may form stable Gd(III) complexes, and DTPA-CIS would probably form the most stable Gd(III) complex of the two.

The positions of PHEA and DO3A in Figure 4 indicate that phenoxy groups are poorer ligating groups than carboxylates in vacuo. A fair comparison of the ligating strength of amides is difficult from this study, since compounds with three amide groups are not included. However, although the bisamides DTPA-BMA and DTPA-HMA have one more ligating atom they seem to be less stable than PHEA, judging from their reaction energies, both in vacuo and in aqueous solution (Table II).

The molecular mechanical calculations used in our study do not consider reaction entropic effects on complex stability. Reaction entropies may differ for complexes that coordinate different numbers of water molecules and for complexes with cyclic ligands compared to open chain ligands. It would be expected that the reaction entropy loss for the ligands is less for the conformationally constrained analogues DTPA-CIS and DTPA-TRANS than for DTPA. The increase in entropy due to loss of coordinated water molecules by complexation of the cation is probably similar for these three compounds, since the complexes coordinate the same number of water molecules. Thus, to the extent that the reaction entropies differ, it seems likely that the reaction entropy will be larger for the cyclic ligands DTPA-CIS and DTPA-TRANS than for the acyclic ligand DTPA, and thus favor complex formation of the two constrained analogues.

Supplementary Material Available: Table of calculated atomic charges (Table III) and a chart (Chart II) showing the adopted atomic labeling convention (12 pages). Ordering information is given on any current masthead page.

(20) Loncin, M. F.; Desreux, J. F.; Merciny, E. *Inorg. Chem.* **1986**, *25*, 2646.

(21) Alsaadi, B. M.; Rossotti, F. J. C.; Williams, R. J. P. *J. Chem. Soc., Dalton Trans.* **1980**, 813.